Supplementary information

Structural Complementarity from DNA for Directing Two-Dimensional Polydopamine Nanomaterials with Biomedical Applications

Tao Ding, Yuxin Xing, Zhenqiang Wang, Haidi Guan, Liucan Wang, Jixi Zhang,* Kaiyong Cai

Key Laboratory of Biorheological Science and Technology, Ministry of Education, College of Bioengineering, Chongqing University, No. 174 Shazheng Road, Chongqing 400044, China. E-mail: jixizhang@cqu.edu.cn

Table of Contents

A: Experimental Section

1. Chemicals and Materials

Unless otherwise noted, all reagent-grade chemicals were used as received, and distilled water was used for the preparation of all the aqueous solutions. Deoxyribonucleic acid from herring sperm (herring sperm DNA, ~50 bp), deoxyribonucleic acid sodium salt from salmon testes (salmon testes DNA, ~2000 bp) and deoxyribonucleic acid sodium salt from calf thymus (calf thymus DNA, ~20000 bp) were purchased from Sigma-Aldrich. Dopamine hydrochloride (AR, 98%), tris (hydroxymethyl)-aminomethane (Tris, 99.9%), 2-[4-(2-hydroxyethyl)-1-piperazinyl]ethanesulfonic acid (HEPES) and doxorubicin hydrochloride (DOX, AR, 98%) were purchased from Aladdin Industrial Inc. 50bp DNA Ladder (MD108) and λ DNA Hind Ⅲ (MD202) were purchased from TIANGEN Biotech (Beijing) Co., Ltd. SYBR Green Ⅰ(10000×) and SYBR Green Ⅱ(10000×) were purchased from Solarbio Science & Technology Co., Ltd (Beijing, China). Agarose G-10 was purchased from biowest. Nucleic acid dye gel view was purchased from BioTeke Corporation (Beijing, China). Hoechst 33258 and Calcein-AM/PI solution were purchased from Yeasen Biological Technology Co., Ltd (Shanghai, China). Cell counting Kit-8 (CCK-8) was purchased from Dojindo Chemical (Shanghai, China). The DOX resistant breast adenocarcinoma MCF-7 cell lines (MCF-7/ADR) were purchased from Bogoo Biological Technology Co., Ltd (Shanghai, China).

2. Characterization

Atomic force microscope (AFM) measurement was performed on an MFP-3D-BIO system (Asylum Research, US). Transmission electron microscopy (TEM) and scanning transmission electron microscopy (STEM) images were obtained using a Talos F200S (ThermoFisher Scientific, Netherlands) instrument with an acceleration

voltage of 200 kV to observe the size, morphology and integrity of the nanosheets. X-ray diffraction (XRD) was measured on a SuperNova XRD system (Agilent, Poland). Small angle X-ray diffraction pattern was produced on Bruker D8 instrument (Bruker, Germany). X-ray photoelectron spectroscopy (XPS) was recorded on an ESCALAB250Xi system (Thermal Scientific, US). Zeta potentials were measured using a Zetasizer instrument (Malvern, UK). Mass spectra were measured using a fourier transform ion cyclotron resonance mass spectrometer (SolariX, Bruker, Germany). The absorption spectra were measured using an UV-Vis Spectrophotometer (NanoDrop One, Thermo) and fluorescence spectra were obtained using a fluorescence spectrophotometer (RF6000, Shimadzu). Circular dichroism spectra (CD) were acquired in a CHIRASCAN instrument (Applied Photophysics, UK). Melting curves were measured in a CFX96 Touch fluorescent quantitative PCR (Bio-Rad, China). Raman spectra were obtained by a LabRAM HR Evolution instrument (HORIBA Jobin Yvon S.A.S, France). Fluorescence images were acquired in a confocal laser scanning microscopy (TCS SP8, Leica). NIR laser irradiation was produced using an 808 nm laser (Mid-River Company, China). The temperature was recorded on a digital thermometer with a thermocouple probe (HH806AU, OMEGA, USA).

3. Fabrication of DNA-PDA nanoplatelets/sheets

Briefly, DNA (with different length: ~50 bp, 100-250 bp, ~2000 bp, or ~20000 bp) and dopamine hydrochloride (8 mg) were added into 7 mL of Tris (18 mg) solution and stirred for 24 h at room temperature. The weight ratio of DNA/dopamine was ranging from 0.025:1 to 2:1. The final products of the DNA-PDA nanoplatelets/sheets were obtained by dialysis against water.

4. Photothermal Performance of DNA-PDA Nanoplatelets/sheets.

To evaluate *in vitro* photothermal performance, an aqueous suspension of DNA-PDA nanoplatelets/sheets (200, 100, 50, 25 and 10 μg mL^{-1}) was irradiated by an 808 nm

NIR laser for 12 min at a power density of 0.5 W cm^{-2}. Deionized water was analyzed as control, and the corresponding temperature changes were recorded using a digital thermometer with a thermocouple probe. The photothermal stability of the nanoplatelets/sheets was assessed by irradiation with an 808 nm laser (0.5 W cm^{-2}) for 12 min and subsequent cooling to room temperature without irradiation. Three cycles of laser on/off were carried out to evaluate photostability. To determine the photothermal conversion efficiency, a suspension of the nanoplatelets/sheets (50 μg mL^{-1}) was continuously irradiated under an 808 nm laser (0.5 W cm^{-2}). The laser was turned off when the temperature was stabilized, followed by the spontaneous cooling of the solution down to room temperature.

The photothermal conversion efficiency (η) of DNA-PDA nanoplatelets/sheets was determined according to the following equation used in the reported studies.[1-4]

$$\eta = \frac{hS(T_{max} - T_{Surr}) - Q_0}{I(1 - 10^{-A_{808}})} \quad (1)$$

Where η is the heat transfer coefficient, S is the sample container surface area, T_{max} is the steady state maximum temperature of DNA-PDA suspension under laser irradiation, T_{surr} is the ambient room temperature, Q_0 is the background energy input by the solvent and the sample container without the presence of DNA-PDA, I is the laser power (0.5 W cm^{-2}), and A_{808} is the absorbance of DNA-PDA (50 μg mL^{-1}) at 808 nm.

The value of hS was calculated according to the following equation:

$$\tau_s = \frac{\sum_i m_i c_{p,i}}{hS} \quad (2)$$

Where τ_s is the characteristic thermal time and m is the mass and c_p is the heat capacity of each i component of the sample cell. The mass of the nanoplatelets suspension was 1.0 g, and its heat capacity ($c_{p,s}$) was approximated to be 4.187 J g^{-1} K^{-1} (the heat capacity of water). In addition, the mass of the quartz cuvette was 5.5 g, and its heat capacity ($c_{p,c}$) was 0.839 J g^{-1} K^{-1}. In order to obtain the τ_s, a dimensionless driving force temperature, θ is introduced using the maximum system temperature,

$$\theta = \frac{T - T_{surr}}{T_{max} - T_{surr}}$$

(3)

At the cooling period, τ_s could be calculated according to the following expression, where t is the time (in s):

$$t = -\tau_s ln\theta \quad (4)$$

The heat energy (Q_0) of the sample cell and solvent without nanoplatelets was calculated from an independent experiment using the following equation:

$$Q_0 = hS(T_{max} - T_{Surr}) \quad (5)$$

The photothermal conversion efficiency (η) of DNA-PDA nanoplatelets/sheets samples was calculated to be 51% (weight ratio of DNA and dopamine: 0.025:1) and 86% (weight ratio of DNA and dopamine: 1.5:1), respectively.

5. Drug loading and release experiments

To investigate the adsorption kinetics of DOX, 1 mg of nanoplatelets and 2 mL of DOX solution (1 mg mL^{-1}) in HEPES buffer (25 mM, pH 7.4) were mixed by sonication. At different time intervals, the suspension was centrifuged, and 3 μL of the supernatant was withdrawn for UV-Vis determination of the adsorbed amount at 480 nm.

For the determination of the adsorption isotherm of DOX, 1 mg of nanoplatelets/sheets was dispersed in 1 mL of the drug solution in HEPES buffer (25 mM, pH 7.4) with various concentrations (2000, 1000, 600, 400, 200, 100, 50, 20 μg mL^{-1}). The mixture was stirred at room temperature for 48 h, and then centrifuged to collect the drug loaded nanoplatelets/sheets. The amount of drug loaded into nanoplatelets/sheets was calculated by subtracting the mass of the drug in the supernatant from the total mass of the drug in the initial solution.

The DOX release study was conducted as follows. First, DOX loaded nanoplatelets/sheets was dispersed in 2 mL of phosphate buffered saline (PBS, pH 7.4),

or sodium acetate buffer solution (20 mM, pH 5.0) with ionic strength of 150 mM. At the predetermined time intervals, 0.2 mL of solution was withdrawn from the suspension and the amount of the released drug was analyzed by using a UV-Vis spectrophotometer. For keeping a constant volume, 0.2 mL of fresh medium was added after each sampling. All drug release results were averaged with three repeated measurements.

To investigate the effects of the NIR irradiation on the drug release, the suspensions of DOX-loaded nanoplatelets/sheets were irradiated under NIR laser (808 nm, 0.5 W cm^{-2}, 5 min) at every time intervals.

Calculation of the corrected concentration of the released DOX is based on the following equation:

$$C_C = C_t + \frac{v}{V}\sum_{0}^{t-1} C_t \quad (6)$$

Where C_c is the corrected concentration at time t, C_t is the apparent concentration at time t, v is the volume of the sample taken (0.2 mL), and V is the total volume of the release fluid (2 mL).

6. Fluorescence labeling of DNA in the nanoplatelets/sheets.

DNA-PDA nanoplatelets/sheets suspension (1 mL) was mixed with 1 μL of SYBR Green Ⅰ and stirred for 2 h in room temperature. The black suspension was then centrifuged to obtain the SYBR Green Ⅰstained nanoplatelets/sheets. After washing with water for three times, the resultant nanoplatelets/sheets were suspended in water and visualized by confocal microscopy.

7. Cell culture

The DOX resistant breast adenocarcinoma MCF-7 cell lines (MCF-7/ADR) were purchased from Bogoo Biological Technology Co., Ltd (Shanghai, China) and cultured in RPMI1640 supplemented with 10% fetal bovine serum (FBS, BI), 100 U mL^{-1}

penicillin, and 100 U mL^{-1} streptomycin under a humidified atmosphere at 37 ℃ (5% CO_2).

8. Cell uptake (Confocal Fluorescence Imaging)

MCF-7/ADR cells were seeded onto confocal microscopy dishes at a density of 1 × 10^5 cells per dish and allowed to adhere for 24 h. Then, the cells were treated with different method: incubated with DOX solution or DOX loaded nanoplatelets/sheets suspension (DOX: 10 μg mL^{-1}, nanoplatelets/sheets: 50 μg mL^{-1}) for 24 h then irradiated with or without 808 nm laser for 5 minutes. Cell nuclei were stained with Hoechst 33258. Finally, the cells were visualized by a confocal laser scanning microscopy (TCS SP5, Leica).

9. *In vitro* cytotoxicity test

The *in vitro* cytotoxicity of DNA-PDA nanoplatelets and drug loaded nanoplatelets was evaluated by a Cell Counting Kit-8 assay (CCK-8, Dojindo Chemical, Shanghai, China). The MCF-7/ADR cells were seeded in 96-well plates at a density of 5.0×10^3 cells per well and incubated at 37 ℃ for 24 h. Next, the culture medium was replaced with fresh cell culture medium containing varying concentrations of nanoplatelets, DOX solution, or DOX loaded nanoplatelets and the cells were incubated for another 24 h. After that, the cells were washed with PBS for three times and incubated with 10 μL of CCK-8 solution together with 90 μL of fresh medium for 2 h. Finally, the absorbance of each well at 450 nm was measured using a microplate reader (Bio-Rad 680, USA).

10. *In vitro* photothermal ablation of MCF-7/ADR cells

In vitro cytotoxicity of DNA-PDA nanoplatelets toward MCF-7/ADR cells during irradiation with the 808 nm laser was evaluated by the CCK-8 assay as well. Cells were seeded in 96-well plates at a density of 5.0×10^3 cells per well and incubated for 24 h,

then fresh medium containing varied concentrations of DNA-PDA nanoplatelets was added to the cells to replace the old medium. After 24 h of incubation, the RPMI 1640 medium containing residual nanoplatelets was removed, and cells with endocytosed nanoplatelets were rinsed with PBS for three times. The culture medium without additives was added into each well, and cells were continuously irradiated with the 808 nm laser at 0.5 W cm^{-2} for 5 min. The cell viability was subsequently determined by the CCK-8 assay.

11. Live/Dead staining

MCF-7/ADR cells were seeded in 24-well plates at a density of 4×10^4 cells per well and incubated for 24 h. Then, the cells were treated under the following different conditions: incubation with DOX solution, DNA-PDA nanoplatelets, DOX loaded nanoplatelets/sheets suspension (DOX: 40 μg mL^{-1}, nanoplatelets/sheets: 200 μg mL^{-1}) for 24 h, followed by irradiation with a 808 nm laser for 5 min; incubation with RPMI 1640 medium for 24 h and laser irradiation for 5 min. After removal of the medium, the adherent cells were rinsed with PBS for three times and incubated with calcein-AM/PI solution (300 μL) for 30 min. Afterwards, living cells and dead cells were stained with calcein-AM (green fluorescence) and PI (red fluorescence) solution, respectively, and visualized by a confocal laser scanning microscopy.

B: Supplementary Figures

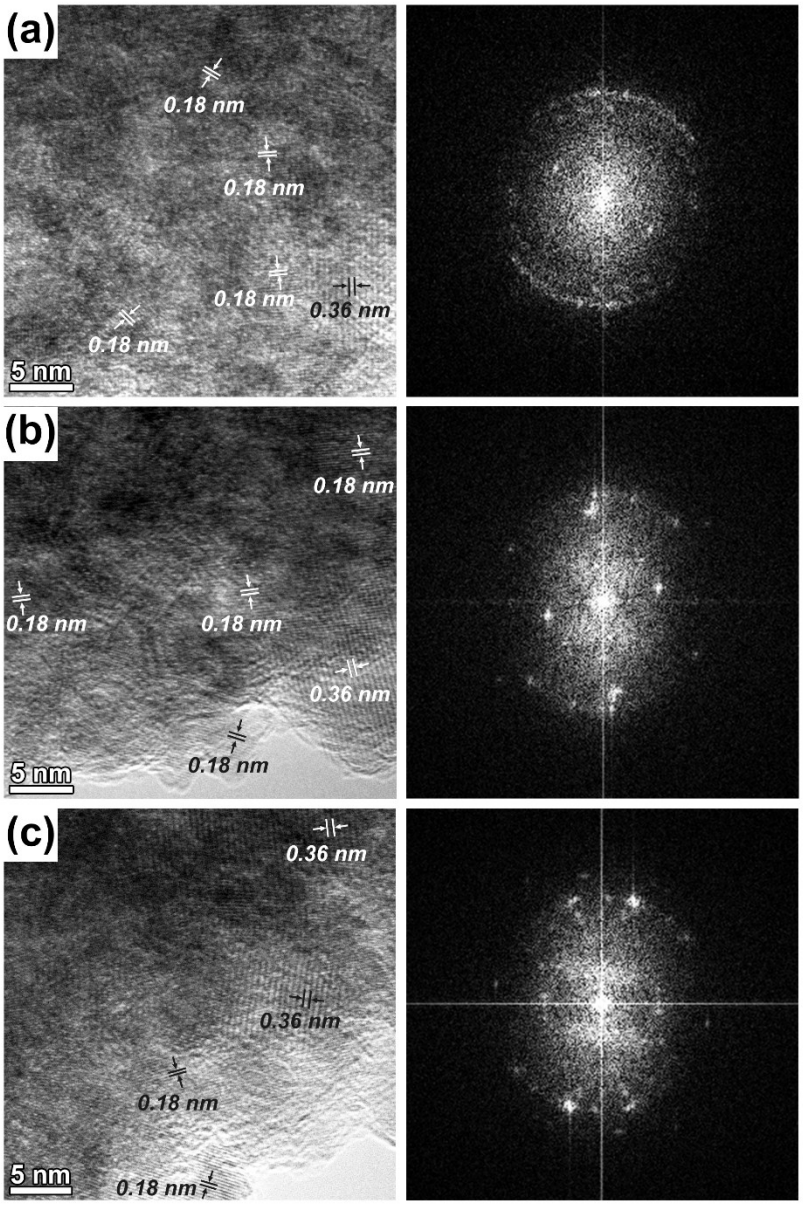

Fig. S1 High-resolution TEM images of DNA-PDA nanoplatelets and corresponding fast Fourier transform (FFT) patterns (a-c).

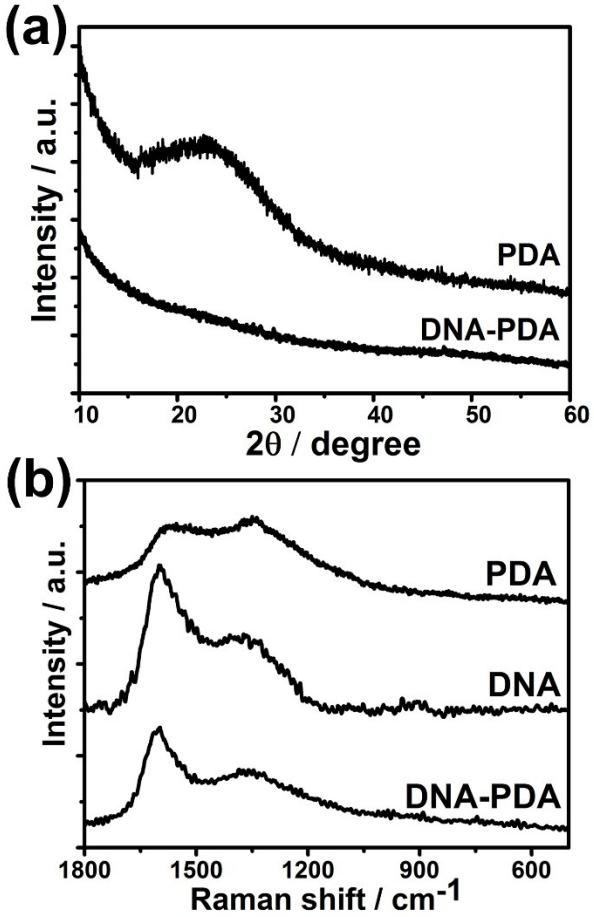

Fig. S2 (a) X-ray diffraction spectra. (b) Raman spectra of DNA, PDA nanoparticles, and DNA-PDA nanoplatelets.

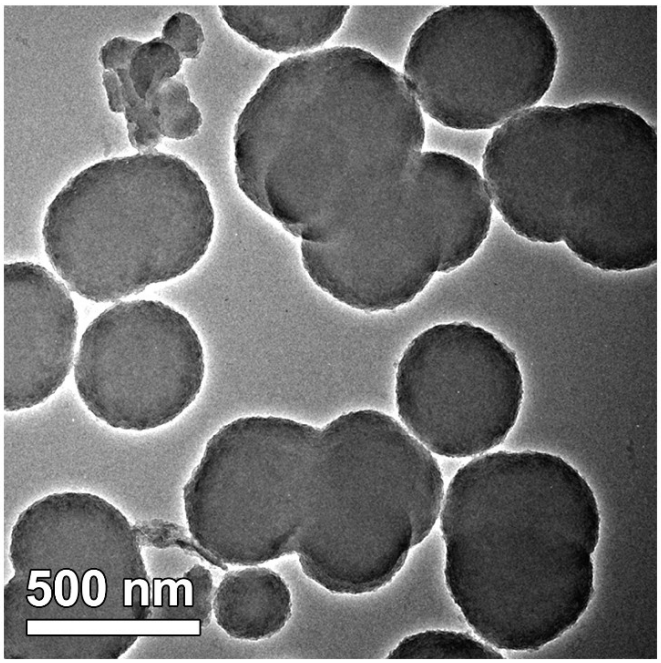

Fig. S3 TEM images of the control polydopamine nanoparticles without the addition of DNA in the synthetic process.

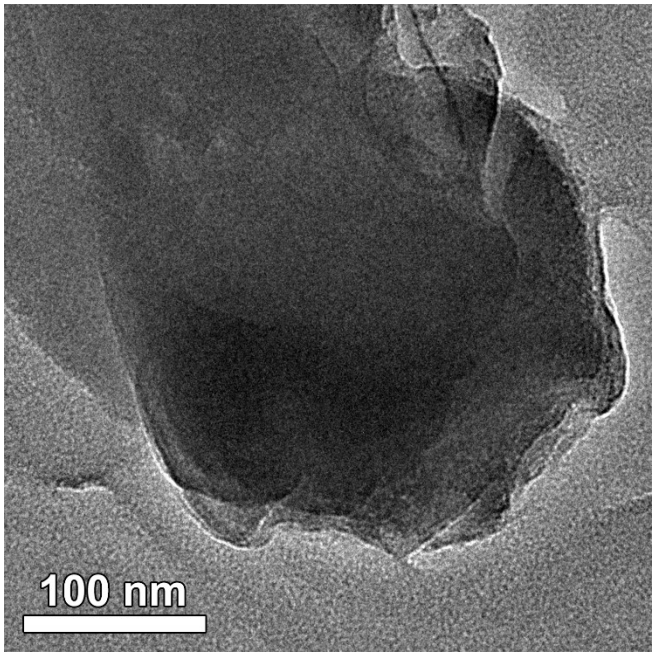

Fig. S4 TEM image of intermediate products from the DNA-PDA nanoplatelets synthesis at the reaction time of 2 h.

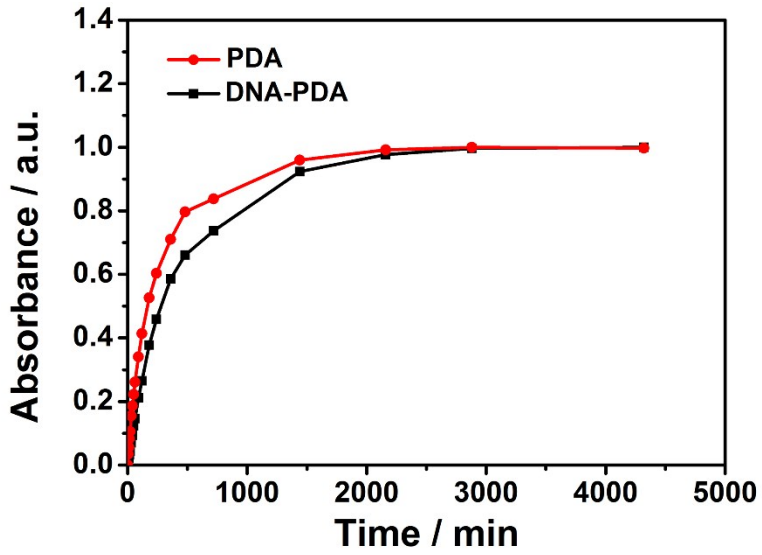

Fig. S5 In situ evolution of PDA polymerization under different conditions by monitoring the absorbance of the synthesis solution at 400 nm over time.

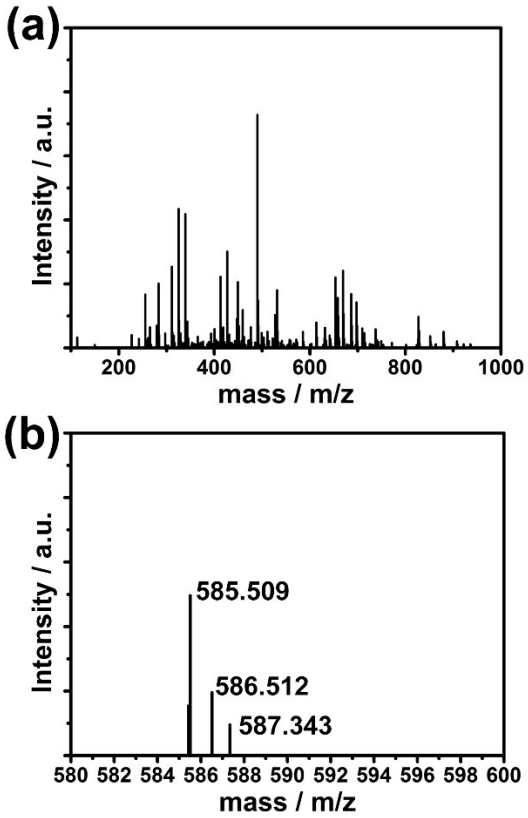

Fig. S6 FT-ICRMS (a) and segmental magnified spectra (b) (m/z 580-600) of DNA-PDA nanoplatelets synthesized at DNA/dopamine weight ratio of 0.025:1.

Three peaks were observed at 585, 586, and 587 Da (corresponding molecular weight was 586, 587 and 588 Da) in the mass spectrum of DNA-PDA nanoplatelets (DNA/dopamine weight ratio of 0.025:1). These peaks were assigned to the cyclic or chain-like tetramer structure, which was in line with previously reported literature.[5-7]

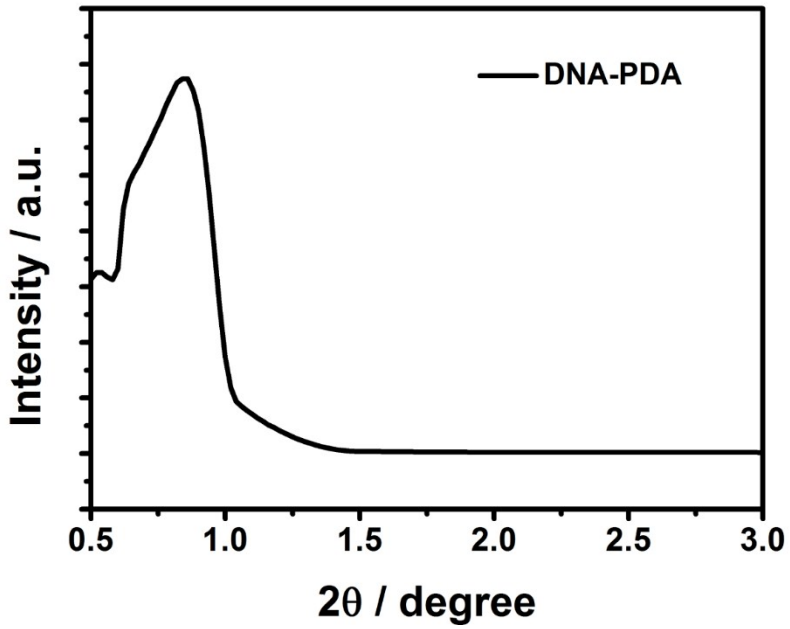

Fig. S7 Small angle XRD pattern of DNA-PDA nanosheets synthesized at an hsDNA/dopamine weight ratio of 1.5:1.

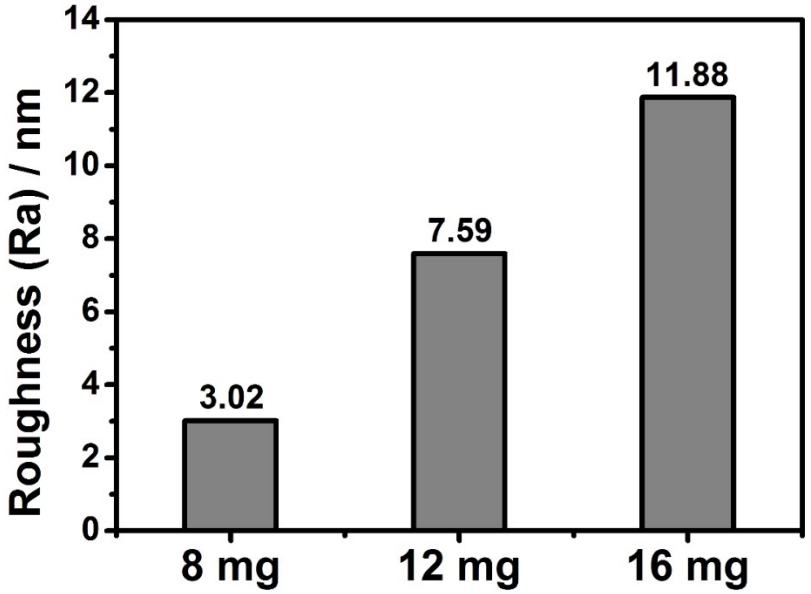

Fig. S8 Surface roughness of DNA-PDA nanosheets synthesized at varying hsDNA/dopamine weight ratios of 1:1, 1.5:1, and 2:1, as obtained by the corresponding AFM images.

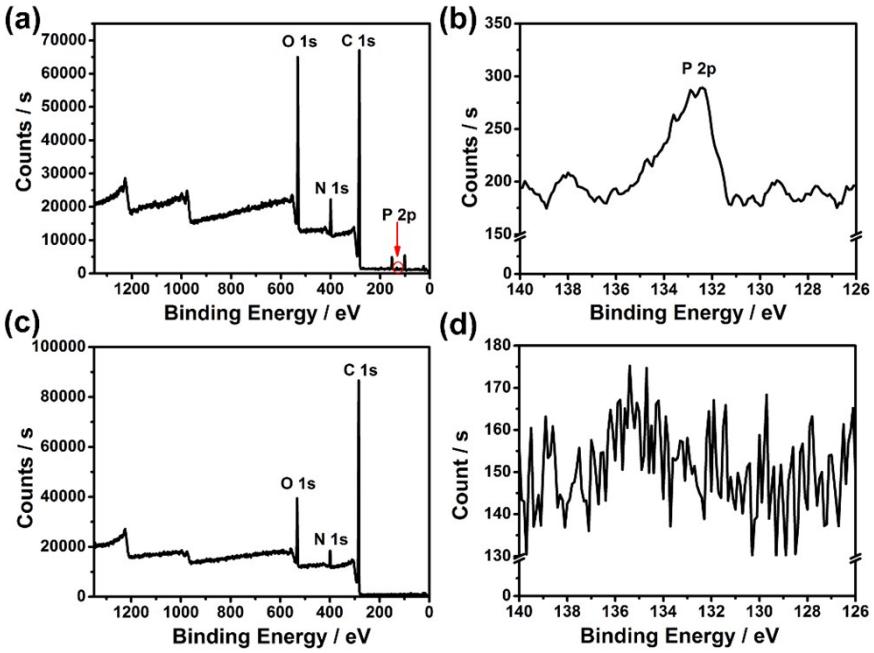

Fig. S9 XPS survey of DNA-PDA nanosheets (a), PDA nanoparticles (c), and corresponding high-resolution scans of P2p peak from the XPS spectra of nanosheets (b) and nanoparticles (d).

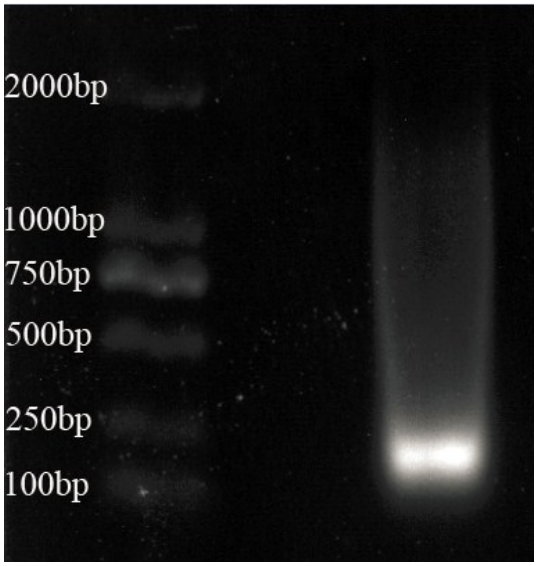

Fig. S10 1% agarose gel electrophoretic separation of sonicated DNA: Lane 1, DL2000 Ladder; Lane 2, DNA sodium salt from Herring testes after sonicated for 20 minutes.

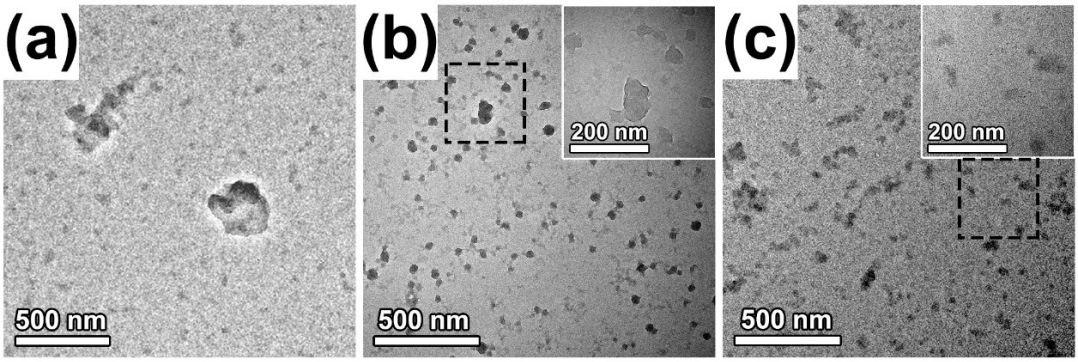

Fig. S11 TEM images of DNA-PDA nanoplatelets synthesized with different DNA: 100-250 bp (a), ~2000 bp (b), and ~20000 bp (c). Magnified images of selected domains in (b) and (c) were presented in the insets.

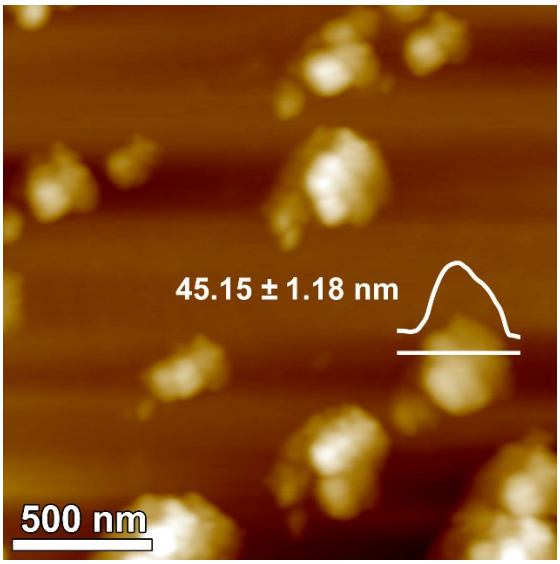

Fig. S12 AFM image of DNA-PDA nanoplatelets synthesized at hsDNA/dopamine weight ratio of 0.025:1. Corresponding height distribution based on the white line in the selected nanoplatelet was shown in the inset.

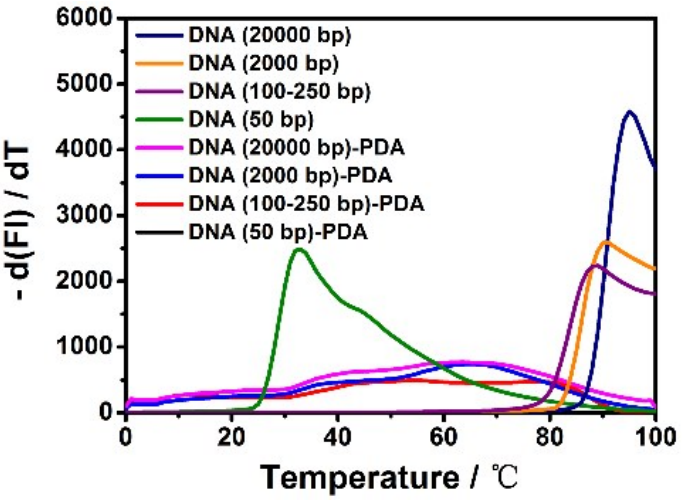

Fig. S13 Melting curves of four different DNA and DNA templated nanoplatelets/sheets.

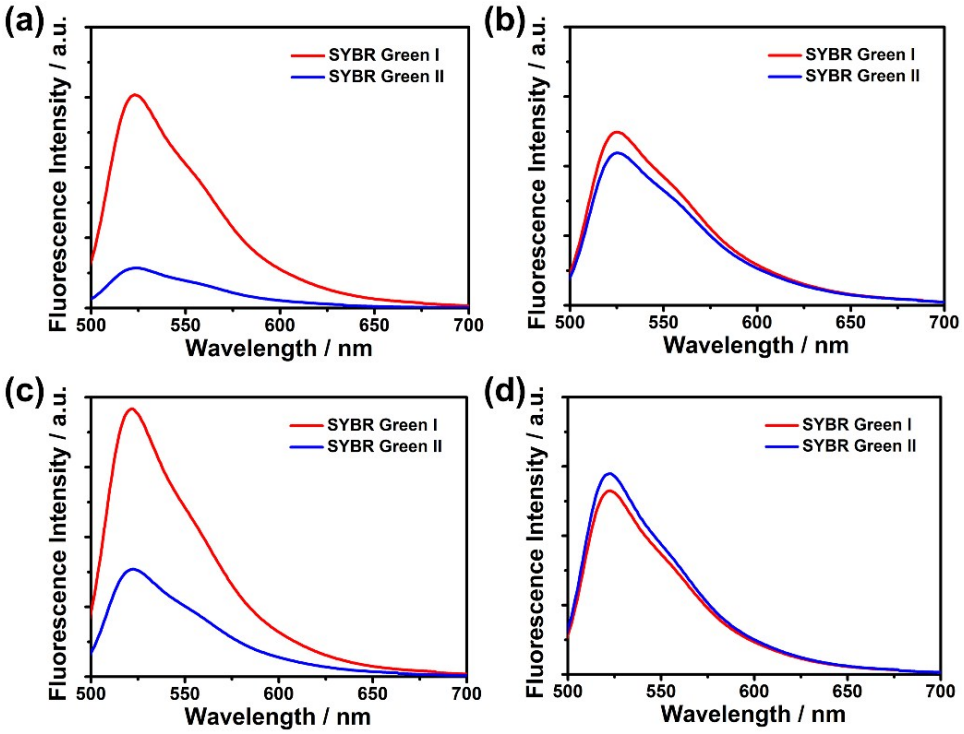

Fig. S14 Fluorescence emission spectra of the supernatant of DNA-PDA nanoplatelets/sheets labeled with SYBR green I and SYBR green II, respectively, aqueous suspension after heated at 60℃ for 10 min. DNA-PDA nanosheets were synthesized at DNA/dopamine weight ratio of 1.5:1.

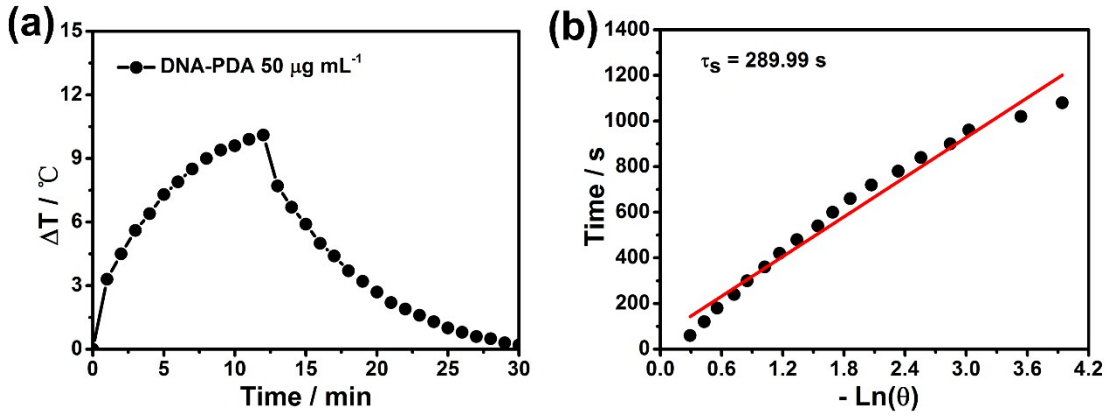

Fig. S15 (a) Photothermal effect of an aqueous dispersion of DNA-PDA nanoplatelets under the irradiation with a NIR laser (808 nm, 0.5 W cm^{-2}) which was turned off after 12 min. (b) Time constant for heat transfer from the system was determined to be 289.99 s by applying the linear time data from the cooling period (after 12 min) *versus* negative natural logarithm of driving force temperature (θ), which was obtained from the cooling stage of figure (a). The DNA-PDA nanoplatelets were synthesized at DNA/dopamine weight ratio of 0.025:1.

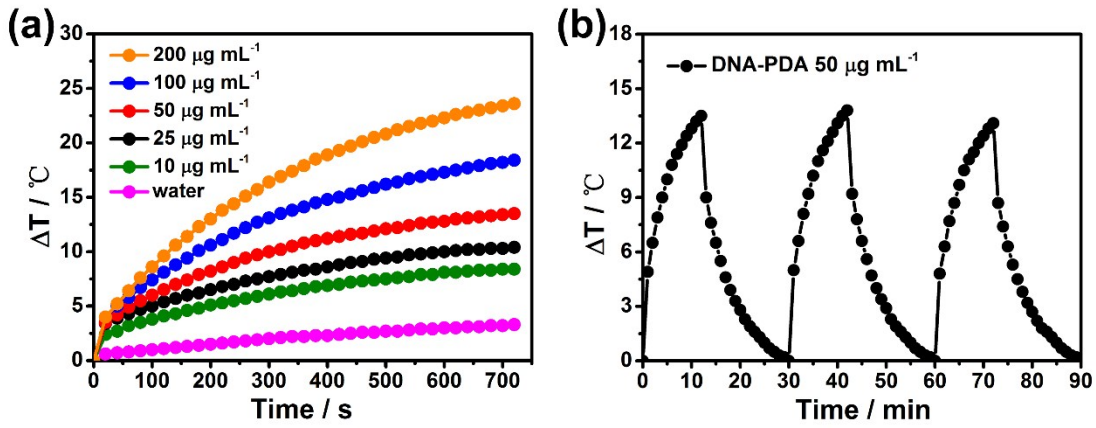

Fig. S16 (a) Photothermal heating curves of aqueous suspensions of DNA-PDA nanosheets (200, 100, 50, 25, 10 μg mL^{-1}, and pure water) during 808 nm laser irradiation (0.5 W cm^{-2}, 12 min). (b) Recycling heating profiles of an aqueous suspensions of nanosheets (50 μg mL^{-1}) under 808 nm laser irradiation (0.5 W cm^{-2}, 12 min) for three laser on/off cycles. The nanosheets were synthesized at DNA/dopamine weight ratio of 1.5:1.

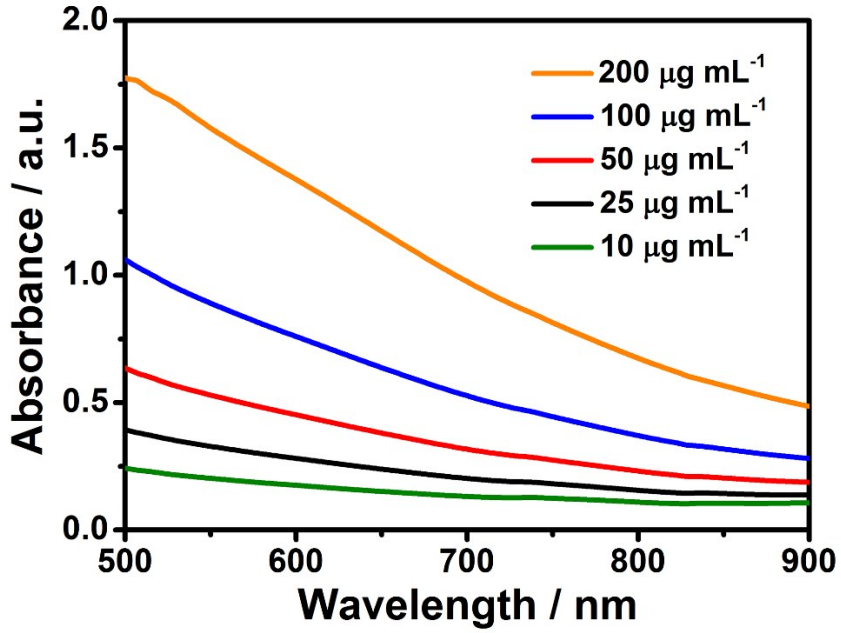

Fig. S17 Absorbance spectra of suspensions of DNA-PDA nanosheets at varying concentrations (200, 100, 50, 25 and 10 μg mL^{-1}). The nanosheets were synthesized at DNA/dopamine weight ratio of 1.5:1.

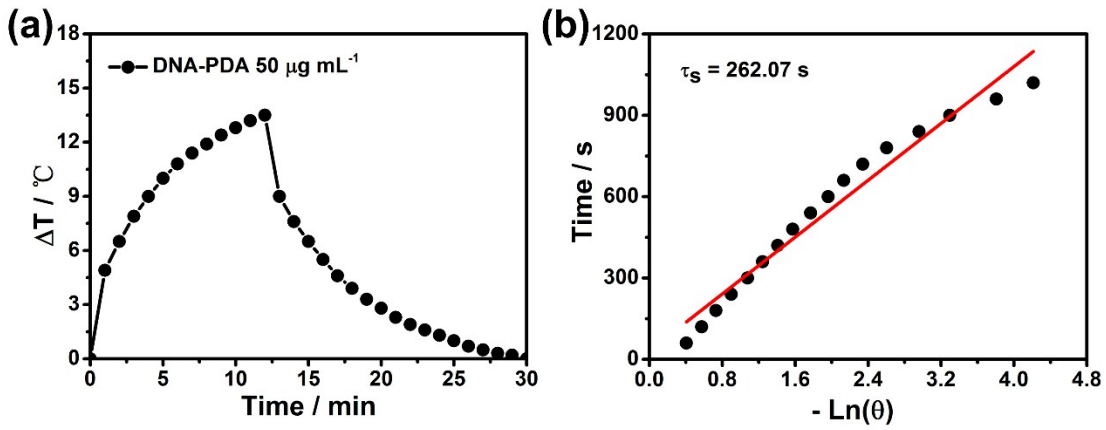

Fig. S18 (a) Photothermal effect of an aqueous dispersion of DNA-PDA nanosheets under the irradiation with a NIR laser (808 nm, 0.5 W cm^{-2}) for 12 min, and then the laser was turned off. (b) Time constant for heat transfer from the system was determined to be 262.07 s by applying the linear time data from the cooling period (after 12 min) *versus* negative natural logarithm of driving force temperature, which was obtained from the cooling stage of figure (a). The nanosheets were synthesized at DNA/dopamine weight ratio of 1.5:1.

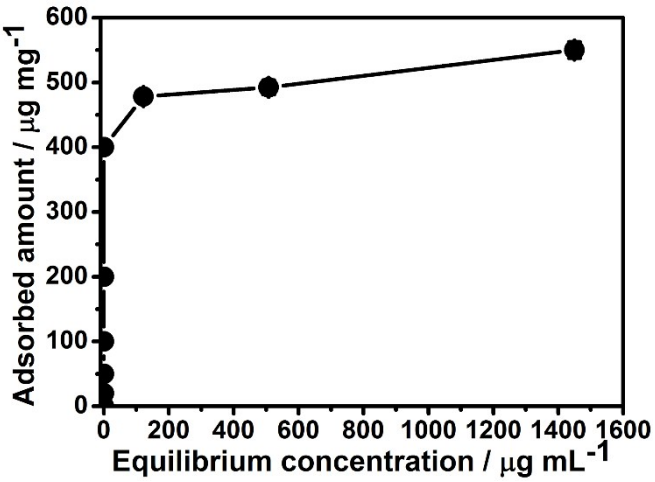

Fig. S19 Adsorption isotherm of DOX on the nanoplatelets.

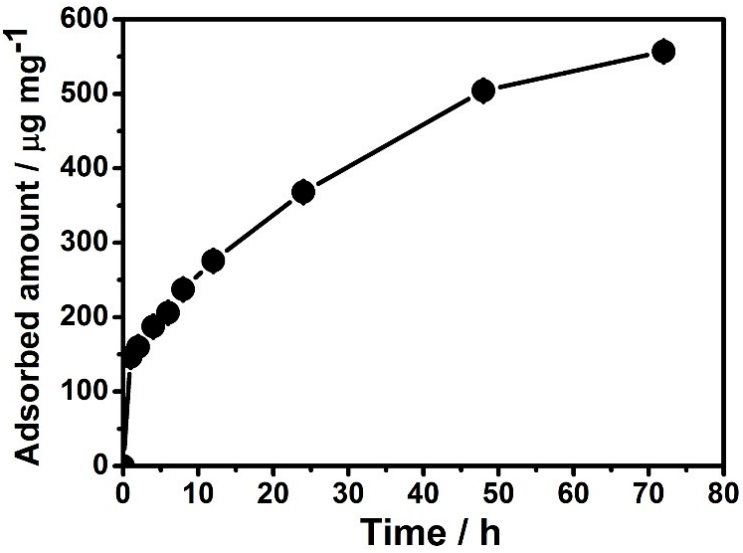

Fig. S20 Adsorption kinetic plot prepared with 1 mg of DNA-PDA nanoplatelets and 2 mL of DOX solution (1 mg mL^{-1}, in HEPES buffer, pH 7.4).

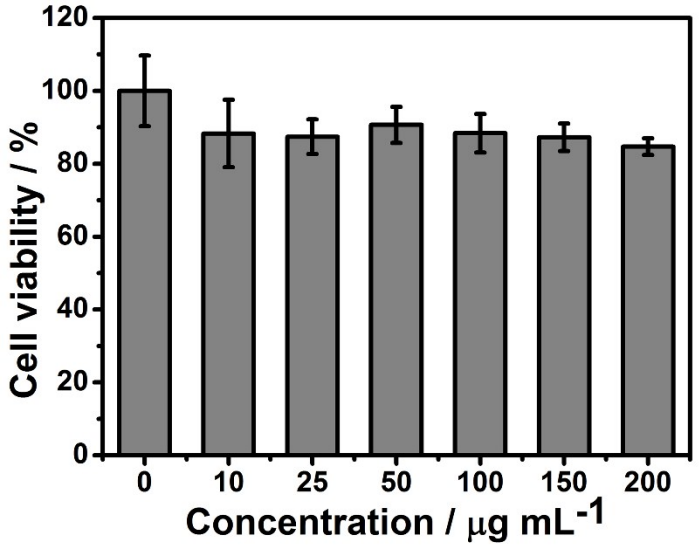

Fig. S21 Relative viabilities of cells after being incubated with nanoplatelets.

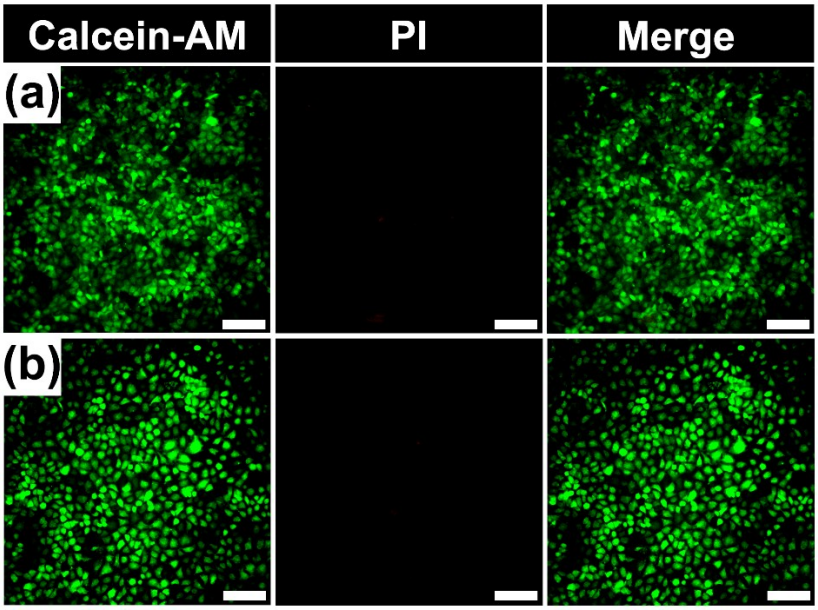

Fig. S22 Fluorescence microscopy images of MCF-7/ADR cells stained with calcein-AM (green, staining living cells) and PI (red, staining dead cells) after different treatments: incubated with DNA-PDA (a) for 24 h, and incubated with culture medium for 24 h, then irradiated with laser for 5 min (b). Concentration of DOX: 40 μg mL^{-1}, concentration of DNA-PDA nanoplatelets: 200 μg mL^{-1}). Scale bar represents 100 μm.

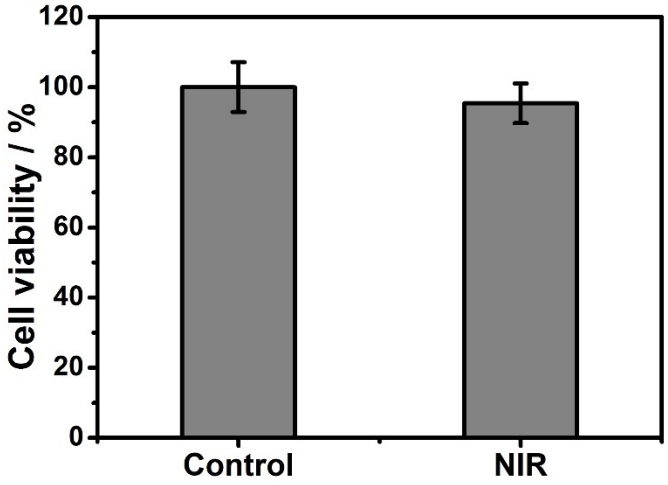

Fig. S23 Relative viabilities of MCF-7/ADR cells after treated with NIR laser only.

References

1 Q. Tian, J. Hu, Y. Zhu, R. Zou, Z. Chen, S. Yang, R. Li, Q. Su, Y. Han and X. Liu, *J. Am. Chem. Soc.*, 2013, **135**, 8571-8577.

2 D. K. Roper, W. Ahn and M. Hoepfner, *J. Phys. Chem. C*, 2007, **111**, 3636-3641.

3 Y. Xing, J. Zhang, F. Chen, J. Liu and K. Cai, *Nanoscale*, 2017, **9**, 8781-8790.

4 C. Ayala-Orozco, C. Urban, M. W. Knight, A. S. Urban, O. Neumann, S. W. Bishnoi, S. Mukherjee, A. M. Goodman, H. Charron, T. Mitchell, M. Shea, R. Roy, S. Nanda, R. Schiff, N. J. Halas and A. Joshi, *ACS Nano*, 2014, **8**, 6372-6381.

5 H. Fan, X. Yu, Y. Liu, Z. Shi, H. Liu, Z. Nie, D. Wu and Z. Jin, *Soft Matter*, 2015, **11**, 4621-4629.

6 M. d'Ischia, A. Napolitano, A. Pezzella, P. Meredith and T. Sarna, *Angew. Chem. Int. Ed.*, 2009, **48**, 3914-3921.

7 S. Meng and E. Kaxiras, *Biophys. J.*, 2008, **94**, 2095-2105.